# Mergers as the Maintenance Mechanism of Cutoff Lows: A Case Study over Europe in July 2021

**Koryu Yamamoto**[1*], Keita Iga[1], and Akira Yamazaki[2]

1. Atmosphere and Ocean Research Institute (AORI), The University of Tokyo
2. Japan Agency for Marine-Earth Science and Technology (JAMSTEC)

*Corresponding Author
Kashiwanoha 5-1-5, Kashiwa, Chiba, Japan 277-8564
koryuy@aori.u-tokyo.ac.jp

« Abstract of this Poster
For further details, Yamamoto et al. (2024, MWR) »

EGU24-14720

## 1. Introduction

**Cutoff Lows** 》
- Detached from troughs
- Accompanied by cold air mass

**A Case in July 2021 (Europe)** 》
- A cutoff low (hereafter, **C1**) caused severe rainfall
- 200+ people dead
- Merger with another cutoff low (hereafter, **C2**)
  → **Maintenance of C1?**

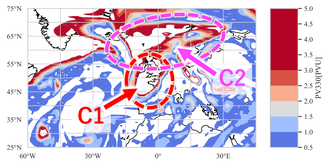


Fig. 1. PV (Potential Vorticity) on 330 K isentropic surface at 0600 UTC 12 July 2021. ERA5 is used for this figure.

**The main aims of the present study are to discuss:**
- the relative contribution of the merger in the maintenance of C1;
- the role of diabatic PV modification during the merger (Few studies have not investigated this aspect yet) .

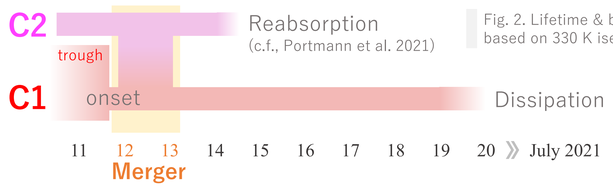


Fig. 2. Lifetime & behaviour of C1 & C2 based on 330 K isentropic surface.

## 2. Data

**ERA5** (Hersbach et al. 2020) 》
- $\Delta x = 0.25^\circ$ & $\Delta t = 1$ [h]
- Used in § 3

**WRF-ARW v.4.4** (Skamarock et al. 2019) 》
- $\Delta x = 20$ [km] & $\Delta t = 60$ [s]
- Used in § 4 & 5

Table 1. Calculation settings with WRF in the present study.

| | |
|---|---|
| Initial Time | 0000 UTC 10 July |
| Domain | Single |
| Initial & Boundary | ERA5 (Hersbach et al. 2020) |
| Microphysics | WSM6 (Hong and Lim 2006) |
| Cumulus | Grell-Freitas (Grell & Freitas 2014) |
| Radiation | RRTMG (Iacono et al. 2008) |
| Planetary Boundary Layer | MYNN 2.5 (Nakanishi & Niino 2006) |
| Land Surface | Noah land-surface model |

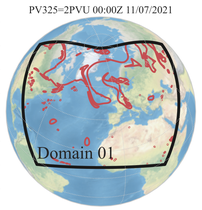


Fig. 3. (black) A domain for the calculation, and (red) 2 PVU isoline at 325 K at 0000 UTC 11 July 2021.

## 3. EKE Budget Analysis

**EKE (Eddy Kinetic Energy) Budget Analysis** 》
- To confirm the inflow from **C2**
- Analyze each component of EKE based on Eq. (1):

(Orlanski & Katzfey 1991; Chang 2000)

$$\left\langle \frac{\partial K'}{\partial t} \right\rangle = -\langle \nabla \cdot (\boldsymbol{V} K') \rangle - \langle \nabla \cdot (\boldsymbol{V}'_a \phi') \rangle - \langle \omega' \alpha' \rangle$$
[rhs1] KFC | [2] AFC | [3] Baroclinic Term
$$- \left\langle \boldsymbol{V}' \cdot (\boldsymbol{V}'_3 \cdot \nabla_3) \overline{\boldsymbol{V}} - \boldsymbol{V}' \cdot \overline{(\boldsymbol{V}'_3 \cdot \nabla_3) \boldsymbol{V}'} \right\rangle$$
[4] Barotropic Term (Reynolds Stress)
$$- [\omega K']\big|_B + [\omega K']\big|_T - [\omega' \phi']\big|_B + [\omega' \phi']\big|_T$$
[5–8] Vertical Flux Convergence of Energy
$$+ \langle \mathrm{RES} \rangle \qquad (1)$$
[9] Residual

- bar: JJA 2021 mean; prime: eddy (defined as deviation)
- subscript "3": 3D; vector without subscripts: 2D
- $K'$: EKE; $\boldsymbol{V}'_a$: eddy ageostrophic wind; $\phi$: geopotential; $\omega$: omega; $\alpha$: specific volume
- $\langle \cdot \rangle$: mean in V (100–900 hPa); $[\cdot]$: mean in S (within 1,000 km from the center of C1)

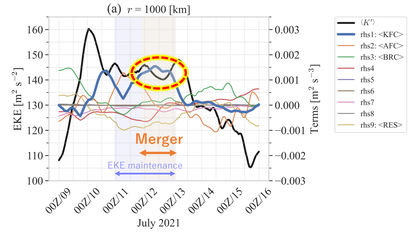


Fig. 4. Temporal evolution of (black line) **EKE** averaged in V and (color line) right-hand terms of Eq. (1). EKE (rhs1–9) is shown in the left (right) vertical axis.

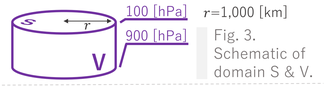


$r$=1,000 [km]

Fig. 3. Schematic of domain S & V.

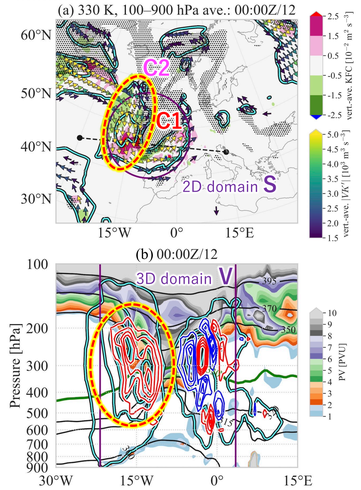


Fig. 5. (a) (color) **KFC**, (cyan contour) **EKE** (100, 300, ..., 1100 $m^2\ s^{-2}$), and (vector) $\boldsymbol{V}K'$ averaged over 100–900 hPa. (hatch) PV330 > 2 PVU.

(b) Cross sections along the black dashed line in (a). (color) PV, (green & black contour) $\theta$, (cyan contour) **EKE** (the same value as (a)), and (red & blue contour) **KFC** ($\pm 0.100$, $\pm 0.075$, $\pm 0.050$, & $\pm 0.025$ $m^2\ s^{-3}$; red shows positive).

Fig. 4 》 • The **EKE** maintenance: 11–13 July
- Although **AFC** (Ageostrophic Flux Convergence) is dominant at first, the later **KFC** (EKE Flux Convergence) dominance **coincides with the merger**.

Fig. 5 》 • **C2 is suggested to be an energetic source.**

## 4. Trajectories

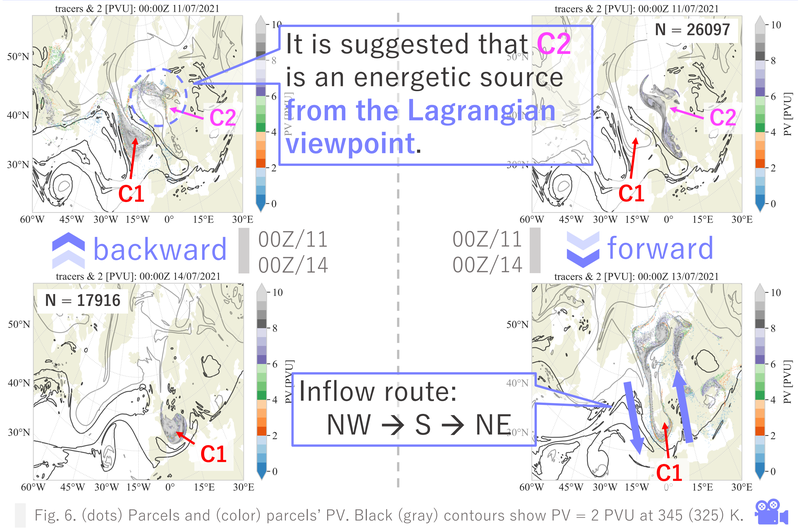


Fig. 6. (dots) Parcels and (color) parcels' PV. Black (gray) contours show PV = 2 PVU at 345 (325) K.

## 5. Diabatic Processes

**The Material Evolution of PV** 》 (Hoskins et al. 1985)

$$\frac{\mathrm{D}}{\mathrm{Dt}}\mathrm{PV} = \frac{1}{\rho}\boldsymbol{\eta} \cdot \nabla\dot{\theta} + \frac{1}{\rho}(\nabla \times \boldsymbol{F}) \cdot \nabla\theta \qquad (2)$$
Diabatic Heating | Forcing

$$\dot{\theta} = \dot{\theta}_C + \dot{\theta}_R + \dot{\theta}_B \qquad (3)$$
All Heating | Latent Heat Release | Radiation | Planetary Boundary Layer

- $\rho$: density; $\boldsymbol{\eta}$: absolute vorticity; $\theta$: potential temperature; $\boldsymbol{F}$: nonconservative forces
- $\dot{\theta} \equiv \mathrm{D(PV)/Dt}$

- Estimate each diabatic term as PV tendency (PVT) along the forward trajectories ( § 4)

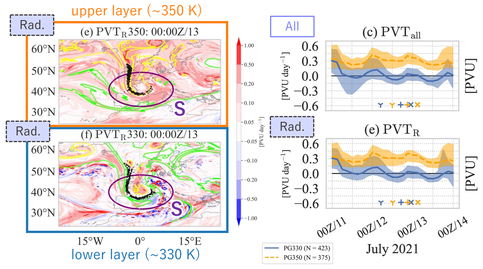


Fig. 7 (←).
(color) PVT by radiation and (black dot) parcels. Lime green (yellow) contours show 2 (8) PVU.

Fig. 8 (→).
PVT of **upper (~350 K)** & **lower (~330 K)** parcel groups (PG). Color line (shading) shows the median (12.5–87.5 %-ile). Symbols indicate the time when the proportion of parcels that penetrate S first exceeds 25% (Y), 50% (+), & 75% (×).

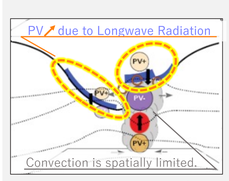


(Portmann et al. 2018)

- The upper parcels (~350 K)
  - obtain **PV↗ due to longwave radiation**
- The lower parcels (~330 K)
  - move into C1 **quasi-adiabatically**

## ■ Summary: a schematic of the merger process

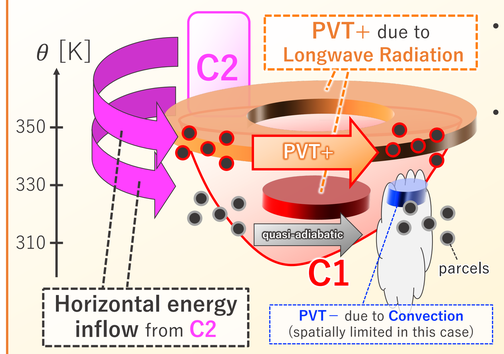


- We confirm that the **merger** with **C2** maintains the intensity of **C1**.
- We suggest different **diabatic PV modification mechanism** depending on the vertical layers during the merger.
  - The upper layer PVT+ enhances the energetic inflow? (i.e., positive feedback of interaction)
    → future study

**References**

Chang, E. K. M., 2000, Mon. Wea. Rev., 128, 25–50.
Grell, G. A. & S. R. Freitas, 2014, Atmos. Chem. Phys., 14, 5233–5250.
Hersbach, H., et al., 2020, Q. J. R. Meteorol. Soc., 146, 1999–2049.
Hong, S.-Y. & J.-O. J. Lim, 2006, J. Korean Meteorol. Soc., 42, 129–151.
Hoskins, B. J., et al., 1985, Q. J. R. Meteorol. Soc., 111, 877–946.
Iacono, M. J., et al., 2008, J. Geophys. Res., 113, D13103.
Nakanishi, M., H. Niino, 2006, Boundary-Layer Meteorol., 119, 397–407.
Orlanski, I. & J. Katzfey, 1991, J. Atmos. Sci., 48, 1972–1998.
Portmann, R., et al., 2018, Q. J. R. Meteorol. Soc., 144, 701–719.
Portmann, R., et al., 2021, Weather Clim. Dynam., 2, 507–534.
Skamarock, W. C., et al., 2019, NCAR Tech. Note, 145 pp.
Yamamoto, K., et al., 2024, Mon. Wea. Rev., accepted.